

# Semiparametric estimation for time series: a frequency domain approach based on optimal transportation theory

Manon FELIX

Advisor: Professor Davide LA VECCHIA

June 2021

## Abstract

In this master thesis, we make use of some results available in the optimal transportation literature to develop a new methodology for parameters estimation in time series models. The key idea is to use the Wasserstein distance and Sinkhorn divergence to derive minimum distance (or divergence) estimators for short- and long-memory time series models. Working on the (discrete) Fourier transform of a time series we conduct inference in the frequency domain. We compute the distance/divergence between the empirical distribution of the standardized periodogram ordinates and their theoretical distribution, as implied by standard asymptotic theory. To study the properties of these new estimators, we perform several Monte-Carlo simulations. Our numerical results suggest that the estimators belonging to our new class are root- $n$  consistent. Their performance, in terms of Mean Squared-Error, is similar to the one yielded by the state-of-the-art estimation method (Whittle's estimator) in the case of short- and long-memory Gaussian process. For short-memory processes and long-memory processes, in the presence of outliers, our estimators outperform the Whittle's estimator as well as when the underlying innovation density of a long-memory process is skewed.

# Contents

<b>1</b>	<b>Introduction</b>	<b>3</b>
1.1	Motivation . . . . .	3
1.2	Organization . . . . .	4
<b>2</b>	<b>Measure transportation</b>	<b>4</b>
<b>3</b>	<b>Inference in the frequency domain</b>	<b>6</b>
<b>4</b>	<b>Methodology</b>	<b>8</b>
4.1	Problem settings . . . . .	8
4.2	Estimation methods . . . . .	9
4.2.1	Minimum Wasserstein Estimator . . . . .	9
4.2.2	Option A: Mean of Minimum Wasserstein Estimators . . . . .	12
4.2.3	Option B: Minimum Semidiscrete Wasserstein Estimator . . . . .	12
4.2.4	Minimum Weighted Wasserstein Estimator . . . . .	13
4.2.5	Minimum Sinkhorn Estimator . . . . .	16
<b>5</b>	<b>Results</b>	<b>17</b>
5.1	Monte Carlo Simulations . . . . .	17
5.1.1	Long-memory Process . . . . .	18
5.1.2	Heavy tailed and Skewed Distribution . . . . .	20
5.1.3	Additive Outliers : Long-Memory . . . . .	23
5.1.4	Short-memory Process . . . . .	24
5.1.5	Additive Outliers : Short-Memory . . . . .	28
<b>6</b>	<b>Conclusion</b>	<b>29</b>
	<b>References</b>	<b>30</b>

# 1 Introduction

## 1.1 Motivation

The aim of this master thesis is to combine some results from optimal transport theory with the statistical analysis of time series analysis. Working with the frequency domain approach, we aim at developing a new methodology for estimating the parameters of a univariate stochastic process.

We do not rely on the standard information divergence-based methods, among which the standard maximum likelihood estimator approach, and consider instead the mathematical theory of optimal measure transportation.

The optimal transport theory has been applied in many research areas, like e.g. mathematics, differential geometry, partial differential equations and applied mathematics (see e.g. [Santambrogio \(2015\)](#) and [Villani \(2009\)](#)). The Wasserstein distance is also useful for contrasting complex objects and can be applied to signal processes and engineering (see e.g. [Kolouri et al. \(2017\)](#)). Many data analysis techniques in computer vision, imaging (e.g. for color/texture processing or histograms comparisons), and more general machine learning problems about regression, classification, and generative modeling are often based on optimal transportation theory (see [Peyré, Cuturi, and others \(2019\)](#)). For an overview on the statistical use of the optimal transportation see [Panaretos and Zemel \(2020\)](#) and for a book-length discussion see [Ambrosio and Gigli \(2013\)](#). Recently, the Wasserstein distance become popular specially for inference in generative adversarial networks (see e.g., [Arjovsky, Chintala, and Bottou \(2017\)](#)).

However, to the best of our knowledge, only a limited number of papers has been investigating the use of the optimal transport theory in the statistical analysis of time series analysis (see [Ni et al. \(2020\)](#)); we refer to [Bernton et al. \(2019\)](#) for a survey of the Wasserstein distance for statistical inference. Our purpose is to fill this gap in the literature and study the applicability of the Wasserstein distance (but not only, with some results from optimal transportation theory) for the statistical analysis of time series, via frequency domain techniques.

The key argument for moving from the time domain to the frequency domain is that we are dealing with data that are independent and identically distributed (i.i.d). The assumption of i.i.d. data facilitates, as it is often the case in statistics, the estimation of parameter(s) in a model.

We propose a new class of minimum distance estimator (see e.g. [Basu, Shioya, and Park \(2019\)](#))

for a book-length introduction) by minimizing the distance between the theoretical and empirical distribution of the standardized periodogram ordinates (SPOs). This program is supported by the fact that the method to replace the maximum likelihood estimator with minimum Wasserstein distance has already been applied, for instance in astronomy and climate science (see [Bernton et al. \(2019\)](#)). Additionally, consistency properties of estimators based on the Wasserstein distance has already been studied by [Bassetti, Bodini, and Regazzini \(2006\)](#) and [Bernton et al. \(2019\)](#).

In our case, we study the properties (bias, variance, consistency, etc.) of our new estimators by means of Monte-Carlo experiments and compare them to the state-of-the-art estimator, the Whittle's estimator (see [Whittle \(1953\)](#)). We analyze our results for several types of distributions (standard, heavy-tailed and skewed) and focus on both large and small samples. We believe that our results are promising and open the possibility for further research.

## 1.2 Organization

The thesis has the following structure. In the first chapter, we review the main concepts of the optimal transport theory and provide the definitions and key mathematical tools necessary to understand our methodological development. In the second chapter, we briefly recall the Whittle's estimation theory and the key related results. Then, we introduce our new estimators and compare them to the Whittle's estimator. We conclude mentioning some potential research which can make use of this thesis as a stepping stone. The R-codes needed to reproduce the exercises/plots/tables included in this thesis are available on Github at the link [https://github.com/ManonFelix/Semiparametric\\_estimation\\_ts](https://github.com/ManonFelix/Semiparametric_estimation_ts).

## 2 Measure transportation

This chapter aims to explain the main principles behind the theory of optimal transport. The original formulation of the optimal transport problem was given by [Monge \(1781\)](#). He proposed a way to calculate the most effective strategy for moving a large amount of sand from one place to another with the least amount of effort required. In mathematical terms, given a source measure  $\mu$ , target measure  $\nu$  supported on sets  $X$  and  $Y$  respectively and a transportation cost function  $c(x, y)$  the goal is to find a transport map  $T : X \rightarrow Y$  such as

$$\min_{\nu=T_{\#}\mu} \int_X c(x, T(x)) d\nu(x)$$

where the constraint  $\mu(T^{-1}(A)) = \nu(A) \implies \nu = T_{\#}\mu, \forall A$  ensures that all the mass from  $\mu$  is transported to  $\nu$  by the map  $T$ .

The notation  $\nu = T_{\#}\mu$  means that the map  $T$  pushes forward  $\mu$  to a new measure  $\nu$  and therefore  $T_{\#}$  is called the pushforward operator.

Monges problem (defined using  $c(x, y) = |x - y|$ ) remained open until the 1940 s, when it was revisited by [Kantorovich \(1942\)](#). In his reformulation, he seeks for a transport plan and allows mass splitting. Therefore, he proposed to compute how much mass gets moved from  $x$  to  $y$  and define a joint measure (a coupling)  $\pi \in \mathcal{P}(\mathbb{R}^d, \mathbb{R}^d)$  which satisfies for all  $A, B \in \mathcal{B}(\mathbb{R}^d)$ :  $\pi(A \times \mathbb{R}^d) = \mu(A)$ ,  $\pi(\mathbb{R}^d \times B) = \nu(B)$ . We denote by  $\Pi(\mu, \nu)$  the set of transport plans between  $\mu$  and  $\nu$  (i.e. couplings). Then,  $p$ -Wasserstein distance is defined as

$$W_p(\mu, \nu) = \left( \min_{\pi \in \Pi(\mu, \nu)} \int_{\mathbb{R}^d \times \mathbb{R}^d} |x - y|^p d\pi(x, y) \right)^{\frac{1}{p}}. \quad (1)$$

Obtaining a closed-form expression for  $W_p$  is typically impossible. However, the case of one dimensional probability densities, say  $f_S(x)$  and  $f_T(x)$  with cumulative distribution functions  $F_S(x)$  and  $F_T(x)$ , is specifically interesting as the  $p = 1$  Wasserstein distance (a.k.a the Earth Mover's Distance, henceforth EMD) has the following expression

$$\mathcal{W}_1(\mu, \nu) = \int_{\mathbb{R}} |F_S(x) - F_T(x)| dx \quad (2)$$

The possibility of using this closed-form solution to conduct inference on time series motivates the thesis.

Beyond the EMD, other transportation measures can be explored to conducted inference. In this thesis we consider the version of the Wasserstein distance:

$$W_{\lambda}(\mu, \nu) = \int_{x, y} c(x, y) d\pi(x, y) + \lambda \int \log \left( \frac{\pi(x, y)}{d\mu(x) d\nu(y)} \right) d\pi(x, y). \quad (3)$$

as introduced by [Cuturi \(2013\)](#). Minimizing Eq. 3 leads to the Sinkhorn divergence. This divergence is obtained adding to the original optimal transportation problem an entropic regularization term (right part). When  $\lambda$  is small, the Sinkhorn divergence approximates the Wasserstein distance.

However, in contrast to the Wasserstein distance, the regularized Sinkhorn divergence is differentiable and smooth, so it yields some computational advantages in terms of optimization problems.

### 3 Inference in the frequency domain

Before introducing our estimators, let us first provide an overview of the theory that is commonly applied to conduct inference on time series models in the frequency domain.

Consider a stationary process  $\{Y_t\}$  of  $n$  observations  $y_{1:n} = y_1, \dots, y_n$ . We focus on linear time series  $\{Y_t\}$  satisfying

$$\phi(L)(1 - L)^d Y_t = \varphi(L)\epsilon_t$$

where  $LX_t = X_{t-1}$  (back shift operator).  $\phi(z)$  and  $\varphi(z)$  are the auto-regressive and moving average polynomial of order  $p$  and  $q$  respectively. The time series  $\{Y_t\}$  may or may not have long memory depending on the value of  $d$ . When  $0 < d < 0.5$  the process is called a long-memory process and are extensively applied in finance (see e.g. [Tsay \(2005\)](#)). In the literature, we often rewrite  $d$  as  $H = d + 1/2$ , which is called the Hurst exponent.

Our setting is of *semiparametric nature*: we have an Euclidean parameter  $\theta$  characterizing the auto-regressive and moving average polynomials and the long memory, but we do not assume any distribution for the innovation term  $\epsilon_t$  (so the innovation density is an infinite dimensional nuisance parameter). For the sake on numerical illustration, we present our results when  $\epsilon_t \sim N(0, \sigma_\epsilon^2 = 1)$  but also underlying innovation densities with fatter tails (like e.g. Skew t (see [Azzalini and Capitanio \(2003\)](#)) and Student t).

To conduct inference on the model parameters  $\theta = (\sigma_\epsilon^2, d, \phi_1, \dots, \phi_p, \varphi_1, \dots, \varphi_q)$  of long-memory processes, we could assume that  $\epsilon_t$  is normally distributed and rely on pseudo (or quasi) MLE. Thanks to this assumption, we can write the likelihood of the process and optimize it to find  $\hat{\theta}$ , which under suitable assumptions remains root- $n$  consistent and asymptotically normal; see e.g. [Gourieroux and Monfort \(1995\)](#). Nevertheless, this approach is extremely time-consuming and can even be unfeasible due to the strong dependence and long-memory properties of the process.

A solution to this inference issue relies on tackling the problem in the frequency domain and work on the discrete Fourier transform of  $\{Y_t\}$ . This is the frequency domain proposed by Whittle and

the key idea is to represent a time series as combination of cos/sinusoids.

The main tool utilized in the frequency domain is the spectral density. The spectral density  $f(\lambda_j, \theta)$  of  $Y_t$  is defined as

$$f(\lambda_j, \theta) = \left| 1 - e^{i\lambda} \right|^{-2d} \frac{\sigma_\epsilon^2 |\varphi(\exp\{-i\omega\})|^2}{2\pi |\phi(\exp\{-i\omega\})|^2}$$

where  $\varphi(x) = 1 - \sum_{k=1}^p \varphi_k x^k$  and  $\phi(x) = 1 + \sum_{k=1}^q \phi_k x^k$ .  $\lambda_j$  are the fundamental Fourier frequencies where  $\lambda_j = 2\pi(j/n)$ ,  $j \in \mathcal{J} = \{1, 2, \dots, [(n-1)/2]\}$ .

The spectrum of a time series can be estimated by the method of moment. Its sample analogue is called the periodogram

$$I(\lambda_j) = \frac{1}{2\pi n} \left| \sum_{t=1}^n (Y_t - \bar{Y}_n) e^{it\lambda_j} \right|^2.$$

The periodogram is asymptotically unbiased. Nevertheless, it is an inconsistent estimator; see e.g. [Priestley \(1981\)](#). Moreover, a key result showed by [Priestley \(1981\)](#) and [Brillinger \(2001\)](#) is that the periodogram ordinates are asymptotically independent and exponentially distributed with rate equal to the spectral density. In other words, the standardized periodogram ordinates (henceforth, SPOs) are asymptotically independent and have an exponential distribution with rate one:

$$\frac{I(\lambda_j)}{f(\lambda_j, \theta)} \xrightarrow{d} i.i.d. \text{ Exp}(1).$$

Whittle introduced and exploited ([Whittle \(1953\)](#)), the idea to minimize the Whittle approximated likelihood:

$$L_W(\theta) = \frac{1}{2\pi} \left[ \int_{-\pi}^{\pi} \ln f(\lambda, \theta) d\lambda + \int_{-\pi}^{\pi} \frac{I(\lambda)}{f(\lambda, \theta)} d\lambda \right] \quad (4)$$

which is derived from the fact that the SPOs are asymptotically identically distributed according to an exponential distribution.

To implement the Whittle's estimator, Eq. 4 can be rewritten by separating the variance component from the rest of the parameters vector as

$$L_W(\theta^*) = \sum_{j \in \mathcal{J}} \frac{I(\lambda_j)}{f(\lambda_j, \theta^*)} \quad (5)$$

where  $f(\lambda_j, \theta^*) = 2\pi\sigma_\epsilon^2 f(\lambda_j, \theta^*)$  and  $\theta^* = (1, \eta = (d, \phi_1, \dots, \phi_p, \varphi_1, \dots, \varphi_q))$ . The following minimization problem (which hinges on the notion of concentrated likelihood) can be set up to find Whittle estimator; see e.g. [Beran \(1994\)](#) for a book-length discussion. First, minimize

$$\arg \min_{\eta} L_W(\theta^*) = \arg \min_{\eta} L_W(\eta)$$

which yields to  $\hat{\eta}$ . Then, set

$$\hat{\sigma}_\epsilon^2 = 2\pi L_W(\hat{\eta}).$$

One can prove (see e.g. [Beran \(1994\)](#)) the consistency of the parameter  $\hat{\theta}^*$ . Additionally, the parameter is root- $n$  consistent and converges to a normal distribution. In the case of underlying Gaussian innovation term,  $\hat{\theta}$  achieves the Cramer-Rao lower bound. The Whittle's estimator is routinely applied to long- and short-memory time series, like e.g. ARMA( $p, q$ ) proces, and it is still consistent and asymptotically normal. We therefore use this estimation method as our reference to compare our results with the state-of-the-art methodology.

## 4 Methodology

### 4.1 Problem settings

Our goal is to find the parameter  $\eta = \theta^*$  of a time series model in the parameter space  $\theta^* \in \Theta$  with dimension  $\Theta \subset \mathbb{R}^s$ , with  $s \geq 1$ , that minimizes the distance between the empirical and theoretical cumulative distributions of the SPOs. We denote the distance or divergence used by  $\mathcal{D}$  and write our minimum distance estimator such as

$$\hat{\theta}^* = \arg \min_{\theta^* \in \Theta} \mathcal{D}(\mu, \nu_{\theta^*}).$$

where  $\mu$  is the theoretical exponential distribution and  $\nu_{\theta^*}$  is the empirical distribution of the SPOs.



We denote the SPOs of a time series  $X_1, \dots, X_m$  where  $X \sim \nu_{\theta^*}$ . In our study, several estimators are considered and each of them leads to an estimator.

In our exposition, we redefine  $\mathcal{D}$  in each optimization problem. For instance, when  $\mathcal{D}$  is the Wasserstein distance, we denote the corresponding minimum Wasserstein estimator (MWE) as  $\hat{\theta}_{MWE}^*$ . For the sake of simplicity, we assumed the variance of the innovation term  $\sigma_\epsilon^2$  to be known and equal to one. Hence, our parameter vector to be estimated is  $\theta^* = (d, \phi_1, \dots, \phi_p, \varphi_1, \dots, \varphi_q)$ . In addition to that, we focus first on processes with underlying Gaussian distribution and then extend to other distributions with fatter tails and contaminated by outliers.

## 4.2 Estimation methods

### 4.2.1 Minimum Wasserstein Estimator

The Wasserstein distance when  $p = 1$  is given in Eq. 2 when  $F_\nu = F_{\theta^*}$  is the empirical cumulative distribution of the SPOs, we estimate it by

$$\hat{F}_{\theta^*}(x) = \frac{1}{m} \sum_{j=1}^m \mathbf{1}_{X_j \leq x}$$

where  $X_j(\theta^*) = I(\lambda_j)/f(\lambda_j, \theta^*)$  for  $j = 1, \dots, m$  are the SPOs of a time series process asymptotically independent and exponentially distributed.

To compute  $F_\mu$ , as it is common in machine learning literature about generative models, we initially thought to generate exponential random variables and stack them in a vector ( $Z$ , say). In mathematical terms, for a sample size  $n$ , we generate  $[(n-1)/2] = m$  observations  $z_1, \dots, z_m$  of random variables  $Z_1, \dots, Z_m$  following an exponential distribution with rate one and store them in a vector  $Z$ . Since  $p = 1$  in Eq. 1 and we work on univariate time series, the Wasserstein distance can be approximated by

$$\mathcal{D}(\mu, \nu_{\theta^*}) = \frac{1}{m} \sum_{j=1}^m |x_j - z_j| \quad (6)$$

where  $x_j$  are the SPOs asymptotically exponentially distributed depending on the parameter vector  $\theta^*$  through the spectral density function  $f(\lambda_j, \theta^*)$  and  $z_j$  are the observations generated using

$Z \sim \text{Exp}(1)$ . Minimizing Eq. 6 leads to the minimum Wasserstein estimator noted

$$\hat{\theta}_{MWE}^* = \arg \min_{\theta^*} \mathcal{D}(\mu, \nu_{\theta^*}).$$

Figure 1 displays the Wasserstein loss function of two FARIMA(0,  $d$ , 0) processes. The top plot shows a smooth and concave loss function with a global minimum that has the same value as the Whittle's estimator's. On the other hand, the bottom plot shows a wiggly function around the true value of the parameter.

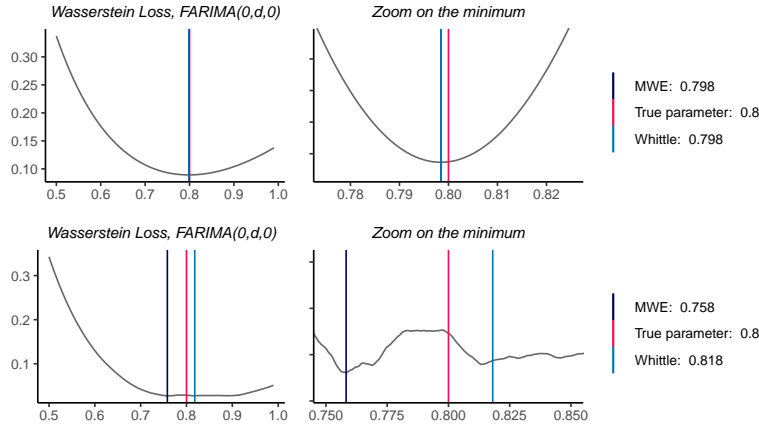


**Figure 1:** Wasserstein loss functions of two FARIMA(0,  $d$ , 0) processes where  $H = 0.8$  ( $d = 1.2$ ). The sample size is 3001. The left column display the entire loss functions for all possible parameter values that a long-memory process can take ( $0.51 < H < 0.99$ ). The right column is a zoom on the functions.

Thus, if one uses the Wasserstein loss to estimate the parameter  $d$ , these two phenomena arise: we end up with either a smooth function containing a global minimum or a function that fluctuates and has several local minima.

Through this thesis, we tackle these issues and introduce estimators that are defined by loss functions which do not suffer from these problems.

Our first finding is that the computed distance might vary widely around the true parameter value and its value depends heavily on the sample simulated from an  $\text{Exp}(1)$ , i.e.  $z_1, \dots, z_m$ . As a consequence, the estimated model parameter(s)  $\hat{\theta}_{MWE}$  typically depends heavily on the random exponential variables generated to conduct the optimization.

To illustrate the problem, on Figure 2 we continue with the process used to plot the bottom plots of Figure 1 and simply change the seed with which the vector  $Z$  is generated. We remark that we are now dealing with a loss function that is smooth and has a global minimum that is precisely

the true value of the parameter  $\theta^* = H = 0.8$ . Therefore, we see that by modifying the vector  $Z$ , we can obtain a more appropriate loss function. We find this aspect potentially problematic for numerical optimization: by definition a random vector cannot be controlled and we may obtain biased estimates simply because of the simulated variables needed for the optimization procedure.

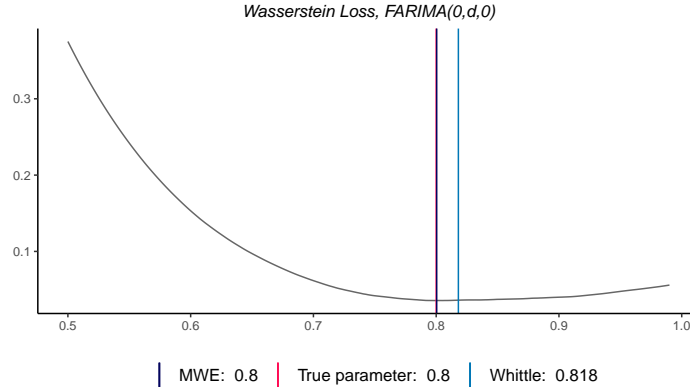


**Figure 2:** *Wasserstein loss function of the FARIMA(0,d,0) process (bottom one) of Figure 1 computed with another random vector.*

In order to get a better overview of the behavior of the minimum Wasserstein estimator when the vector  $Z$  changes, we compute  $k = 200$  times  $\hat{\theta}_{MWE}^*$  for a given process of size  $n = 3001$ . Then, we plot the results on Figure 3. We can observe that, even for large sample size, the estimated parameter depends heavily on the random vector  $Z$ . Nevertheless, the mean remains relatively close to the true value.

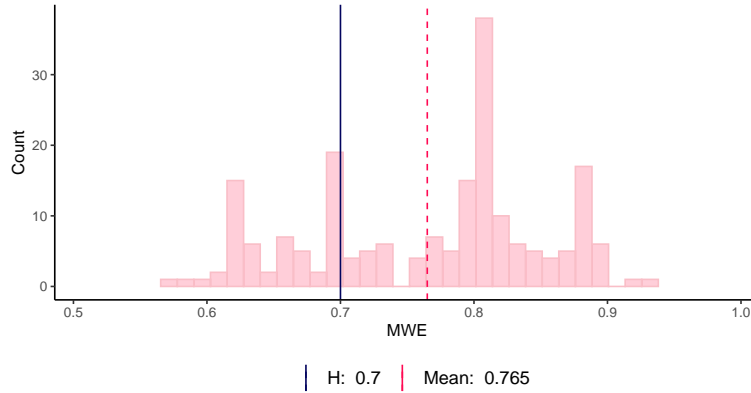


**Figure 3:** *We simulate 200 vectors following an exponential distribution and then compute the MWE of a FARIMA(0,d,0) process with  $n = 3001$ . The blue line is the true parameter  $H = 0.7$  value and the red dashed line is the mean of the MWE.*

To cope with this problem of dependence between the random vector  $Z$  and the parameter estimate, we are going to explore the two following options.

#### 4.2.2 Option A: Mean of Minimum Wasserstein Estimators

For each simulated times series, we generate several exponential random variables and stack them in vectors. Then, we estimate the model parameter for each of the simulated vector and report the mean of the estimated parameter.

For instance, based on the same process than on Figure 3 with  $n = 3001$ , we generate  $k = 10, 20, 50, 100, 200, 500, 1000$  random vectors, estimate the  $k$  parameters and then report the mean. Thus, the mean becomes our estimator and we note it  $\hat{\theta}_{MMWE}^*$ . The results are listed in Table 1. As  $k$  increases, the average becomes progressively closer to the true parameter.

$k$	1	10	20	50	100	200	500	1000
$\hat{\theta}_{MMWE}^*$	0.807	0.73	0.727	0.726	0.721	0.719	0.714	0.714

**Table 1:** Mean of the minimum Wasserstein estimators for a FARIMA(0, d, 0) of size  $n = 3001$  by varying the value of  $k$ , i.e. the number of exponential random vectors generated. The true value is 0.7.

#### 4.2.3 Option B: Minimum Semidiscrete Wasserstein Estimator

Instead of using the empirical cumulative distribution function (c.d.f) of exponential random variables generated from a computer, we plan to use the c.d.f of exponential variables with rate one for the SPOs, namely  $F(x) = 1 - e^{-x}$ . Therefore, the Wasserstein distance becomes:

$$\int_{\mathcal{X}} \left| \hat{F}_{\theta^*}(x) - (1 - e^{-x}) \right| dx \quad (7)$$

where  $\hat{F}_{\theta^*}(x) = \frac{1}{m} \sum_{j=1}^m \mathbf{1}_{X_j \leq x}$  and  $x_j$  are the SPOs of a process. To compute this distance, we replace  $\hat{F}_{\mu}(z) = \frac{1}{m} \sum_{j=1}^m \mathbf{1}_{Z_j \leq z}$  by  $F_{\mu} = 1 - e^{-x}$ . We use a trapezoidal integration to approximate the integral and name the estimator minimum semidiscrete Wasserstein estimator (MSWE). Thanks to this second option, there is no longer randomness in our process estimation. The corresponding loss functions for two FARIMA(0, d, 0) processes using this method are showed on Figure 4

Still, another problem persists. The Wasserstein loss, even for large sample size, is often not well-shaped (i.e smooth and concave): it may contain several local minima (see e.g. Figure 1 and Figure 4). This fact entails biased estimates with large variance.

So far, we are not able to explain why there is such diversity in the shape of the loss functions when the process follows a Gaussian distribution and we are planning to investigate theoretically this point.

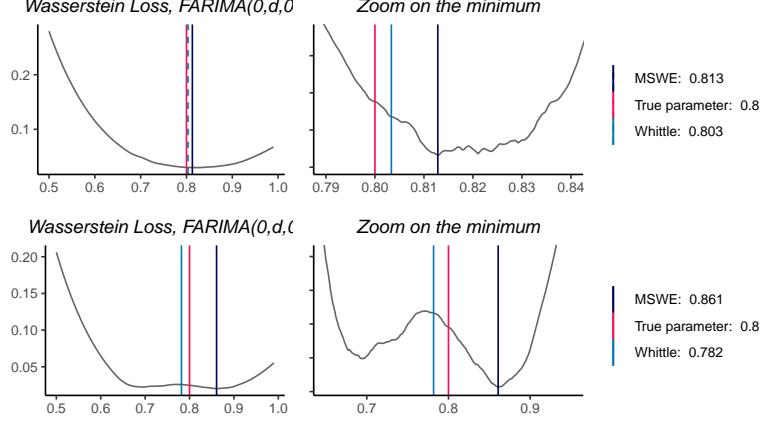


**Figure 4:** Semidiscrete Wasserstein loss functions for two  $\text{FARIMA}(0,d,0)$  processes. The sample size is 3001 and the true parameter value is 0.8.

It should also be noted that the loss shape degenerates even more when  $n$  decreases (see Figure 5).



**Figure 5:** Wasserstein loss function of a  $\text{FARIMA}(0,d,0)$  process with sample size equal to 51.

#### 4.2.4 Minimum Weighted Wasserstein Estimator

In our numerical experiments, we realized that inserting some weight in the loss function defined by the Wasserstein distance yields a much more regular function to optimize. Therefore, we introduce another class of minimum divergence estimators which are related to the minimization problem of Eq. 2 where the empirical cumulative distribution of the SPOs  $\hat{F}_\nu(x) = \hat{F}_{\theta^*}(x)$  is given by

$$\hat{F}_{\theta^*}(x) = \sum_{j=1}^m w_j 1\{X_j \leq x\}$$

where  $X_j(\theta^*) = I(\lambda_j)/f(\lambda_j, \theta^*)$  for  $j = 1, \dots, m$  are the SPOs of a time series process and the associated weights  $\{w_j\}$  are

$$w_j = \frac{\frac{I(\lambda_j)}{f(\lambda_j; \theta)}}{\sum_{j=1}^m \frac{I(\lambda_j)}{f(\lambda_j; \theta)}}. \quad (8)$$

We call the estimator solution to the minimization problem in Eq. 8 the minimum weighted Wasserstein estimator; we will use the acronym MWWE and the notation  $\theta_{MWWE}^*$ .

To implement the MWWE we resort on some optimization routines already available in the statistical software (R). Most of these routines require that the weights sum up to 1 and that are comprised between 0 and 1. Therefore, we propose the use of the weights in Eq. 8.

In order to give an intuition for the employment of these weights, we report on Figure 6 a Quantile-Quantile plot. These are the quantiles of the SPOs of a FARIMA(0,  $d = 0.8, 0$ ) process computed by substituting  $\theta^* = \hat{\theta}_{Whittle}^* = 0.818$  and  $\theta^* = \hat{\theta}_{MWWE}^* = 0.742$  against the quantiles of an exponential distribution with rate one. We notice that the SPOs from the minimum Wasserstein distance estimation method have an heavy tailed distribution than those from Whittle's estimation method (see Figure 6). This phenomenon is not an isolated case and often the Wasserstein's SPOs have this feature. Intuitively, the weights proposed give more leverage to extreme values while computing the Wasserstein distance and therefore prevents the SPOs selected by the Wasserstein distance minimization method from being too extreme in value and too far from an exponential distribution with rate one.

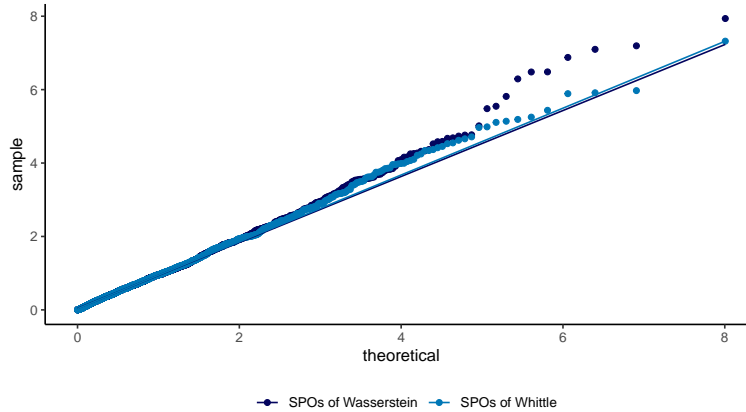


**Figure 6:** *Qqplot of the Wasserstein's SPOs and the Whittle's SPOs. The SPOs are from a long-memory process with  $H = 0.8$  and the sample size is equal to 3001.*

Figure 7 shows the plot of the loss function for same process and vector  $Z$  as Figure 1, but now we apply the weights to calculate our weighted Wasserstein distance. We see that the weighted Wasserstein loss function becomes smooth and contains a minimum which is even closer to the true

parameter than the one obtained optimizing the Whittle's likelihood function.

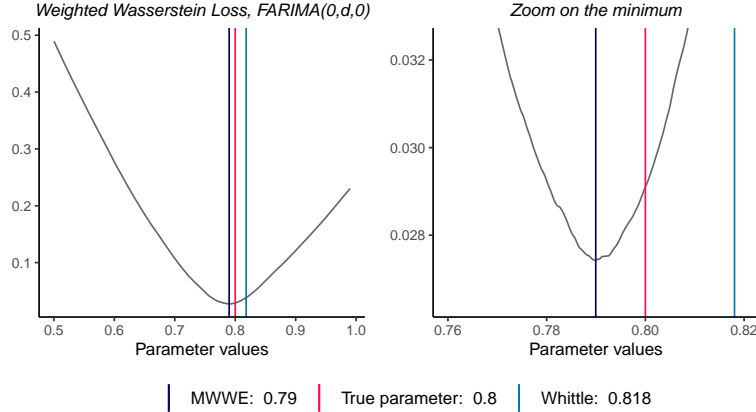


**Figure 7:** *Weighted Wasserstein loss function of the FARIMA(0,d,0) process on Figure 1 (bottom).*

We are aware that the weights applied here are not optimal: the problem of selecting optimal (in some asymptotic sense, like e.g. minimum trace of the asymptotic variance) weights remains open and it will be the object of our future research. Nevertheless, the weights proposed in this section work well especially for ARMA( $p, q$ ) processes as illustrated on Figure 8. The shape of the loss function using the weighted Wasserstein estimator suggests that we could obtain an estimator with small variance—this intuition came from looking at the convexity of the loss function in a neighbourhood of the true parameter value. Moreover, we are also thinking of implementing the minimum expected Wasserstein estimator defined by [Bernton et al. \(2019\)](#). Also this research topic will be investigated in future research.

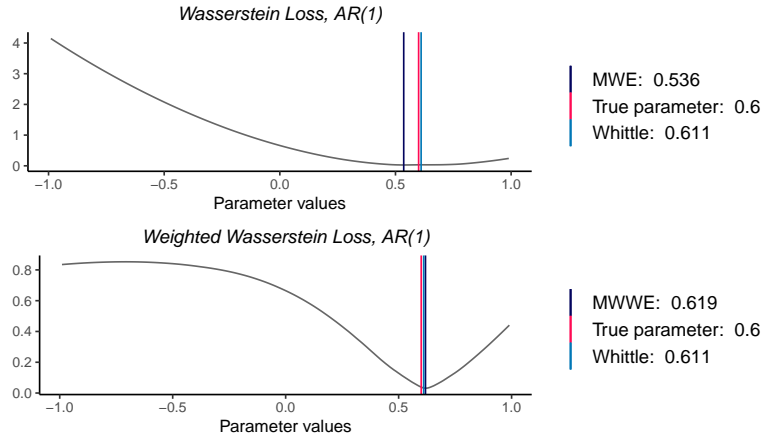


**Figure 8:** *Wasserstein loss function and weighted Wasserstein loss function of a Gaussian AR(1) process. The sample size is 3001 and the true parameter is 0.6.*

#### 4.2.5 Minimum Sinkhorn Estimator

A second idea is to employ the Sinkhorn divergence (see Eq. 3) to estimate our parameter based on Cuturi (2013). We think that the regularization term should have an impact on the shape of the loss function, making it smoother. To check numerically this conjecture, on Figure 9, we compare the loss function of the Wasserstein distance with the one related to the Sinkhorn divergence. We see that we deal with a smooth and concave function, whose minimum is very close to the true value. Another good property of the Sinkhorn divergence is that it remains smooth even for a very small sample size.

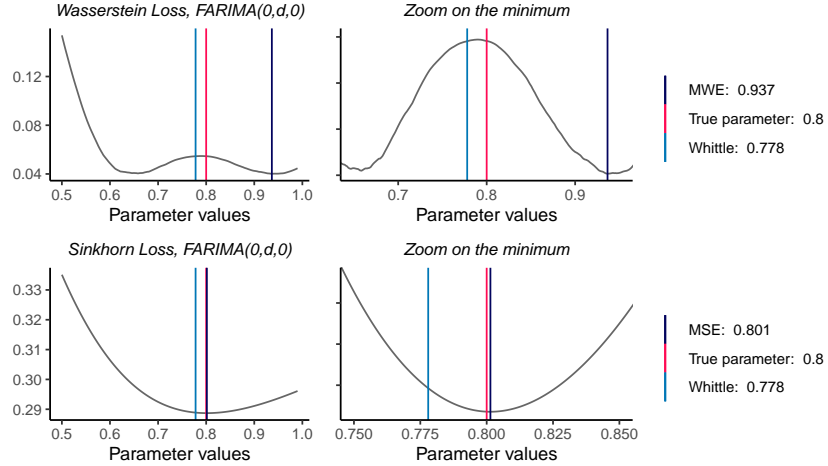


**Figure 9:** Top: Wasserstein loss function of a FARIMA(0,d,0) process. Bottom: Sinkhorn loss function of the same process. The sample size is 1801.

Nevertheless, the use of the Sinkhorn divergence raises an important question: which value(s) to select for  $\lambda$ ? In order to choose the optimal (in a sense that we are going to clarify)  $\lambda$ , we suggest to implement classical machine learning techniques to perform model selection, such as the cross validation (leave-one-out); see for example Friedman et al. (2001) Chapter 7.

To illustrate, we randomly divide a time series into 2 groups  $C_1$  (80%),  $C_2$  (20%) also called folds. We treat the first group as train set and the second group as validation/test set. For a selection of  $\lambda$ , we estimate our parameter, the minimum Sinkhorn estimator (MSKE), on the train set and then use the corresponding  $\hat{\theta}_{MSKE}$  to predict the time data of our test set.

For the sake-of-exposition, we illustrate the procedure using an AR(1) process,  $Y_t = \phi_1 Y_{t-1} + \epsilon_t$  where  $\epsilon_t \sim N(0, 1)$  and  $\theta^* = \phi_1 = 0.6$ . After estimating the parameter thanks to the train set, we substitute its value in  $\hat{\epsilon}_t = Y_t - \hat{\theta}_{MSKE}^* Y_{t-1}$  where  $t = 2, \dots, l$ .  $l$  is the length of the testing vector and depends on which ratios we choose to split our time process  $Y_t$  in our case 80% – 20%. Then,



we compute the empirical prediction error  $err_\lambda$  for a given  $\lambda$ :

$$err_\lambda \text{ of the test set} = \frac{1}{l} \sum_{t=2}^l \hat{\epsilon}_t^2 = \frac{1}{l} \sum_{t=2}^l (Y_t - \hat{\theta}_{MSKE}^* Y_{t-1})^2$$

We repeat this method for several lambda values and plot the results on Figure 10. The minimum testing error is achieved when  $\lambda = 0.1$ , to which corresponds  $\hat{\theta}_{MSKE\lambda=0.1}^* = 0.572$ - a value close to the true parameter value  $\theta^* = 0.6$ .

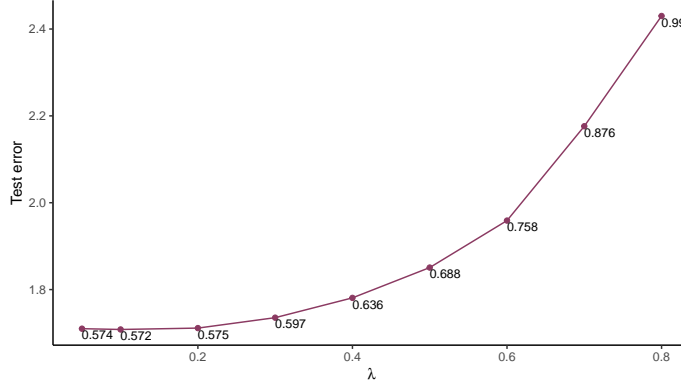


**Figure 10:** Testing MSE vs lambda values for an AR(1) process. The sample size is 4001 and the true parameter value is 0.6. For this process, the minimum empirical prediction error is achieved when lambda = 0.1.

## 5 Results

### 5.1 Monte Carlo Simulations

In this section we run a horse race among the different estimators presented in the previous sections. Our criteria for evaluating the performance of each of the estimators is the Mean Squared Error ( $MSE$ )

$$MSE(\hat{\theta}^*, \theta^*) = \mathbb{E}(\theta^* - \hat{\theta}^*)^2 = \text{Var}(\hat{\theta}^*) + \text{Bias}^2(\hat{\theta}^*, \theta^*)$$

where  $\text{Bias}(\hat{\theta}^*, \theta^*) = \mathbb{E}[\hat{\theta}^*] - \theta^*$  and  $\text{Var}(\hat{\theta}^*) = \mathbb{E}[(\hat{\theta}^*)^2] - \mathbb{E}[\hat{\theta}^*]^2$ . The MSE represents the bias-variance trade-off which typically emerges in statistics when it comes to model selection. To obtain approximations of the MSE, bias and variance of  $\hat{\theta}^*$ , we compute

$$\widehat{MSE}(\hat{\theta}^*, \theta^*) = \frac{1}{B} \sum_{b=1}^B (\hat{\theta}_b^* - \theta^*)^2,$$

$$\widehat{Bias}(\hat{\theta}^*, \theta^*) = \hat{\theta}^{*\cdot} - \theta^*,$$

$$\widehat{Var}(\hat{\theta}^*) = \frac{1}{B-1} \sum_{b=1}^B (\hat{\theta}_b^* - \hat{\theta}^{*\cdot})^2$$

where  $B$  is the number of Monte Carlo simulations, i.e. the number of simulated processes, and  $\hat{\theta}^{*\cdot} = \frac{1}{B} \sum_{b=1}^B \hat{\theta}_b^*$ .

### 5.1.1 Long-memory Process

Firstly, we simulate  $B = 400$  stationary FARIMA(0,  $d$ , 0) processes of size  $n = 3201$  and  $H = 0.8$  ( $d = 0.3$ ) according to

$$(1 - L)^{0.3} Y_t = \epsilon_t.$$

For each process, we compute the Whittle's estimator  $\hat{\theta}_{WH}^*$ , the minimum Wasserstein estimator  $\hat{\theta}_{MWE}^*$ , the mean of the minimum Wasserstein estimators  $\hat{\theta}_{MMWE, k}^*$ , the minimum semidiscrete Wasserstein estimator  $\hat{\theta}_{MSWE}^*$ , the minimum weighted Wasserstein estimator  $\hat{\theta}_{MWWE}^*$  and the minimum Sinkhorn estimator  $\hat{\theta}_{MSKE, \lambda}^*$ . Figure 11 reports the results.

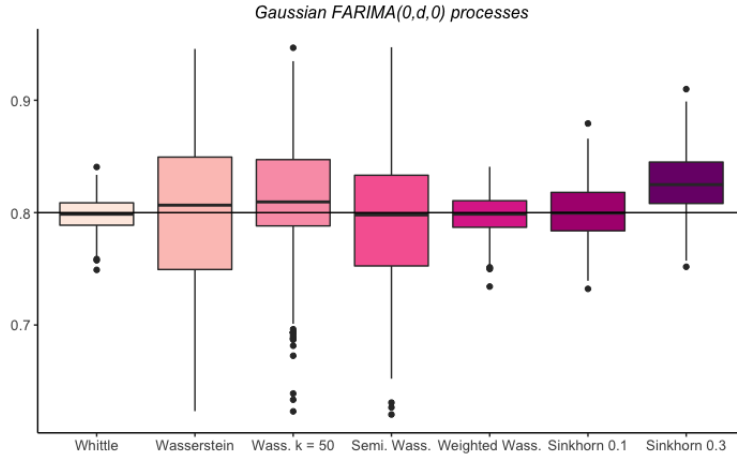


**Figure 11:** Boxplots of all the estimators presented during this thesis. The sample size of the 400 simulated Gaussian FARIMA(0,  $d$ , 0) is 3201 and  $d = 0.3$  ( $H = 0.8$ ).

We note that the minimum Wasserstein estimator has very high variance due to the problems mentioned earlier. By using the mean of the minimum Wasserstein estimators we can reduce the variance and the bias of the minimum Wasserstein estimator (see Table 2) while using the minimum semidiscrete Wasserstein estimator allows to reduce the bias. Our minimum weighted Wasserstein

estimator is similar to Whittle's estimator in terms of Mean Squared Error: both estimators have small variance and a bias close to 0 (see Table 2). We zoom on the density of these two estimators and we display it on Figure 12. We see that both distributions are centered around the true parameter and have similar shape. Nevertheless, the minimum weighted Wasserstein estimator has larger tails, which entails a larger variance.

The use of the Sinkhorn distance seems promising but depends on the  $\lambda$  parameter. When  $\lambda$  is equal to 0.1, the minimum Sinkhorn estimator is well centered around the true parameter and has a reasonable variance. Here, we do not choose  $\lambda$  by cross-validation because of the time needed for computation. We compute the Sinkhorn distance where the value of  $\lambda$  is determined in advance. It is expected that by performing a selection of lambda parameters we will obtain even better results.

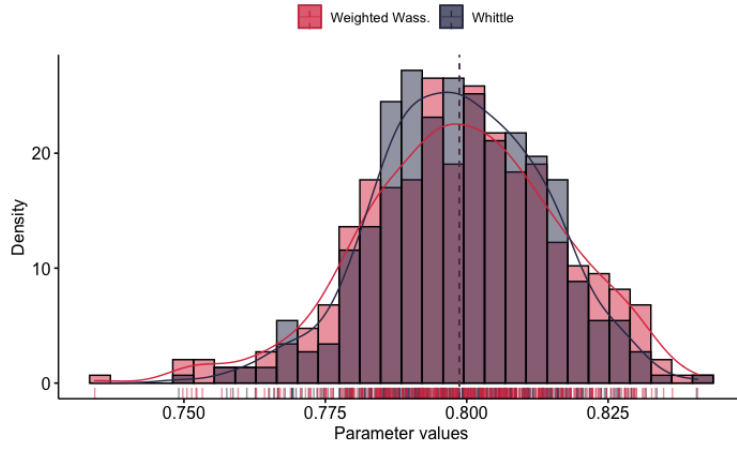


**Figure 12:** Distribution of the Whittle's estimator and the weighted Wasserstein estimator estimated with the 400 simulations of Figure 11.

Distribution	Gaussian		
	$\widehat{MSE}(\hat{\theta}^*)$	$\widehat{Bias}(\hat{\theta}^*)$	$\widehat{Var}(\hat{\theta}^*)$
$\hat{\theta}_{Whittle}^*$	0.00018	-0.00164	0.00018
$\hat{\theta}_{MWE}^*$	0.00425	-0.01207	0.00411
$\hat{\theta}_{MMWE, k=50}^*$	0.00319	0.00930	0.00318
$\hat{\theta}_{MSWE}^*$	0.00452	-0.00327	0.00451
$\hat{\theta}_{MWE}^*$	0.00027	-0.00150	0.00027
$\hat{\theta}_{MSKE, \lambda=0.1}^*$	0.00057	-0.00155	0.00057
$\hat{\theta}_{MSKE, \lambda=0.3}^*$	0.00125	0.02363	0.00069

**Table 2:** Mean Squared Errors, bias and variance of Figure 10.

### 5.1.2 Heavy tailed and Skewed Distribution

Mikosch et al. (1995) showed that the fatter the tails of the innovations distribution, the faster the Whittle's estimator converges to the true parameter value. The first impact of the modification of the kurtosis of the distribution is that the Wasserstein loss function becomes smooth and concave. For instance, the error distribution on Figure 13 is heavy tailed  $\epsilon_t \sim t_4$  and we can observe that the loss is well-shaped and perfectly concave. We also notice that the smoothness is present even for small sample sizes. Therefore, the Whittle's estimator and the minimum Wasserstein estimator are usually very close in value when the underlying distribution has heavier tails than the Gaussian.

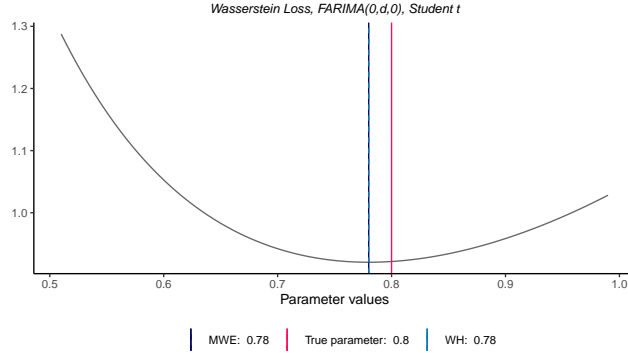


**Figure 13:** Wasserstein loss function of a  $FARIMA(0,d,0)$  process distributed according to a Student  $t$  distribution with degree of freedom equal to 4. The sample size is equal to 3001.

In addition to modifying the excess of kurtosis of a distribution and thus increasing the probability of observing extreme values, we are also interested in observing how our estimators behave when the error distribution is asymmetric. Therefore, we use the skew normal distribution  $SN(\alpha)$  to allow for non-zero skewness by varying the symmetry parameter  $\alpha$  of the distribution. Then, we combine these two descriptive statistics of the error distribution through the skew  $t$  distribution developed by Azzalini and Capitanio (2003). Consequently, the distribution of the innovation term becomes heavy tailed but on top of that skewed.

The skew  $t$  distribution is related to a standard skew normal random variable  $T$  and a random variable  $M$  following a chi-squared distribution with  $v$  degree of freedom by the equation:

$$R = \frac{T}{\sqrt{\frac{M}{v}}}.$$

Then the linear transformation  $X = \mu + \sigma R$  has a skew  $t$  distribution with parameters  $\mu, \sigma, \alpha$ , and  $v$  and the corresponding notation  $ST(\mu = 0, \sigma = 1, \alpha, v)$  to denote the skew  $t$  random variable  $X$ .

For illustration, we plot on Figure 14 densities of skew normal and skew t distribution for some selected values of  $\alpha$  and  $v$ .

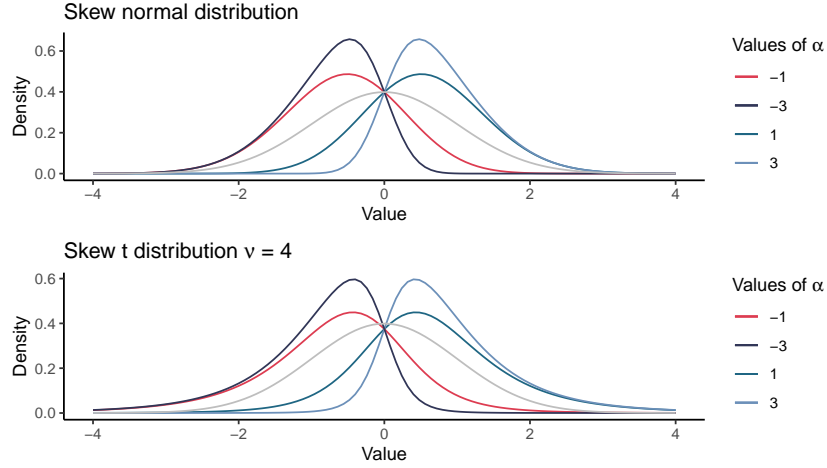


**Figure 14:** Density plot of skew normal and skew t distribution for some selected values of the skewness parameter and the degree of freedom.

In order to compare our estimators fairly in our Monte Carlo simulations, we keep the parameters of these three distributions constant. Therefore, we consider a Student t distribution with a degree of freedom equal to 4, i.e.  $\epsilon_t \sim t_{v=4}$ , a skew normal distribution with shape parameter equal to 1, i.e.  $\epsilon_t \sim SN(\alpha = 1)$  and a skew t distribution combining both of them, i.e.  $\epsilon_t \sim ST(\mu = 0, \sigma = 1, \alpha = 1, v = 4)$ .

We simulate  $B = 400$  FARIMA(0,d,0) processes for each of these three distributions and plot the result on Figure 15.

Let us begin by analyzing what occurs when the distribution is a Student t (top plot of Figure 15). We note that all estimators (apart from those based on the Sinkhorn distance) have a considerably smaller variance than when the process is Gaussian and, consequently, a smaller MSE (see Table 3). For example, the first and third quartile of the minimum semidiscrete Wasserstein estimator are respectively 0.758 and 0.832 in the case of Gaussian processes and becomes 0.788 and 0.8089 when the distribution has heavier tails. The Whittle's estimator remains the leader in terms of MSE.

Then, when the distribution is set to be a skew normal one, we can notice that a bias arises for each estimators (see middle plot of Figure 15). Indeed, all estimators are biased in the sense they overestimate the value of the true parameter. The Whittle's estimator is the second estimator that suffers most from this bias. Our new estimators are more robust and subsequently experience a smaller MSE (see Table 3).

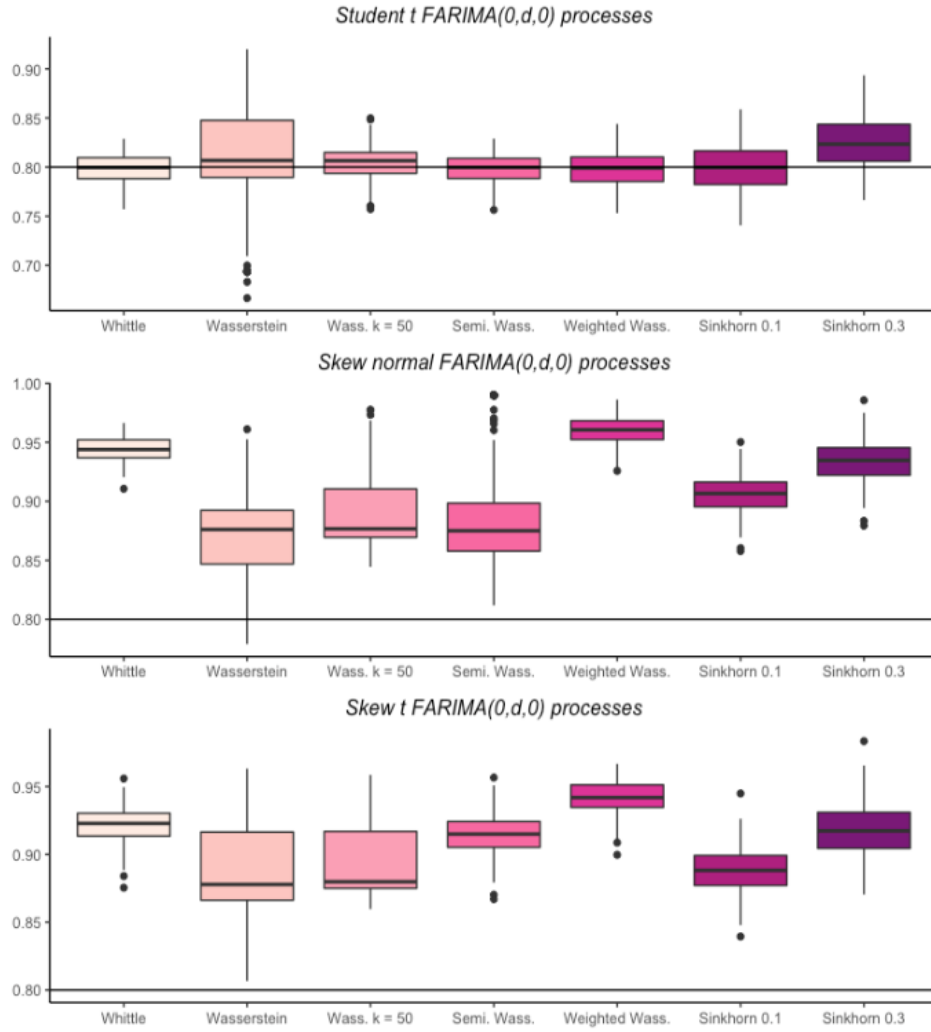


**Figure 15:** Boxplots of all the estimators presented during this thesis. The sample size of the 200 simulated FARIMA(0,d,0) is 3201. From top to bottom the underlying distributions are Student  $t$ , skew normal and skew  $t$ .

<b>FARIMA(0, d = 0.3, 0)</b>	$\widehat{MSE}(\hat{\theta}^*)$	$\widehat{Bias}(\hat{\theta}^*)$	$\widehat{Var}(\hat{\theta}^*)$
<b>Distribution</b>	<b>Student t</b>		
$\hat{\theta}_{Whittle}^*$	0.000211	-0.001675	0.000210
$\hat{\theta}_{MWE}^*$	0.002846	0.012169	0.002712
$\hat{\theta}_{MMWE, k=50}^*$	0.000314	0.003980	0.000300
$\hat{\theta}_{MSWE}^*$	0.000214	-0.001689	0.000212
$\hat{\theta}_{MWWE}^*$	0.000295	-0.002362	0.000290
$\hat{\theta}_{MSKE, \lambda=0.1}^*$	0.000570	-0.000891	0.000572
$\hat{\theta}_{MSKE, \lambda=0.3}^*$	0.001287	0.024379	0.000696
<b>Distribution</b>	<b>Skew normal</b>		
$\hat{\theta}_{Whittle}^*$	0.020847	0.143981	0.000117
$\hat{\theta}_{MWE}^*$	0.006300	0.069800	0.001435
$\hat{\theta}_{MMWE, k=50}^*$	0.009379	0.091769	0.000963
$\hat{\theta}_{MSWE}^*$	0.008979	0.085507	0.001676
$\hat{\theta}_{MWWE}^*$	0.025578	0.159484	0.000144
$\hat{\theta}_{MSKE, \lambda=0.1}^*$	0.011437	0.105650	0.000277
$\hat{\theta}_{MSKE, \lambda=0.3}^*$	0.018244	0.133753	0.000356
<b>Distribution</b>	<b>Skew t</b>		
$\hat{\theta}_{Whittle}^*$	0.014959	0.121619	0.000169
$\hat{\theta}_{MWE}^*$	0.008616	0.087040	0.001045
$\hat{\theta}_{MMWE, k=50}^*$	0.009343	0.093530	0.000598
$\hat{\theta}_{MSWE}^*$	0.013206	0.114045	0.000201
$\hat{\theta}_{MWWE}^*$	0.020252	0.141760	0.000157
$\hat{\theta}_{MSKE, \lambda=0.1}^*$	0.008096	0.088171	0.000324
$\hat{\theta}_{MSKE, \lambda=0.3}^*$	0.014119	0.117058	0.000418

**Table 3:** MSE, bias and variance computed with 200 simulated FARIMA(0,d,0) processes with three different underlying distributions.

Regarding the impact of the skew t distribution, all the MSE are better than when the distribution is simply asymmetric due to the fact that having heavier tails seems to make the estimators converge faster.

To sum up, the estimators based on the Wasserstein distance (except for the minimum weighted Wasserstein estimator) overperform the Whittle's estimator when the underlying distribution of the innovation terms is skewed.

### 5.1.3 Additive Outliers : Long-Memory

In this section we are interested in the influence of occasional outliers in our new estimators. It appears that in the case of Gaussian FARIMA(0, d, 0) some of our estimators (in particular, the one

based on weighted Wasserstein distance) seem to overperform Whittle’s estimator in terms of MSE. To demonstrate this propriety we simulate  $B = 200$  FARIMA(0,  $d$ , 0) contaminated by occasional isolated outliers. The Gaussian processes  $\{Y_t\}$  are distributed according to

$$Y_t = (1 - W_t) X_t + W_t (c \cdot V_t)$$

where  $W_t \sim \text{Bern}(p)$ ,  $V_t \sim t_2$  and  $c = 10$ . In Table 4, we report the ratio between the MSE / bias / variance of the Whittle’s estimator and the minimum weighted Wasserstein estimator for different values of  $p = 0, 0.001, 0.01, 0.05$  (when  $p = 0$  the process is not contaminated by outliers). The results suggest that when the time series is contaminated, the minimum weighted Wasserstein estimator overperform the Whittle’s estimator in terms of MSE. Indeed, as soon as we introduce noise the ratio becomes greater than 1. For a  $p < 0.01$ , we improve the bias and the variance thanks to the weights and when  $p \geq 0.01$  our gain exclusively comes from the bias.

p	0	0.001	0.01	0.05
MSE ratio	0.682	1.208	1.105	1.012
Bias ratio	0.104	1.000	1.054	1.010
Variance ratio	0.686	1.206	0.991	0.8128

**Table 4:** MSE / Bias / Variance of the Whittle’s estimator divided by the MSE / bias / variance of the MWWE. The number of simulated time series is equal to 200 with sample size equal to 3001. The innovation terms are distributed according to a standard normal distribution.

#### 5.1.4 Short-memory Process

We also aim to demonstrate the performance of our estimators for short-memory processes. To do this, we simulate  $B = 200$  auto-regressive processes of order 2 according to:

$$Y_t = 0.75Y_{t-1} - 0.25Y_{t-2} + \epsilon_t.$$

The processes are stationary since the three stationary conditions are met:

1.  $\phi_2 < 1 + \phi_1$
2.  $\phi_2 < 1 - \phi_1$
3.  $\phi_2 > -1$

where  $\phi_1 = 0.75$  and  $\phi_2 = -0.25$ .



We cannot include the Sinkhorn divergence in our comparison because the function used in R requires too much time to calculate this divergence and fails to converge. The results when  $\theta^* \subset \mathbb{R}^2$  are on Figure 16 with corresponding MSE, bias and variance for each estimator in Table 5, 6, 7 and 8. Again, we consider several distributions for  $\epsilon_t$ :  $\epsilon_t \sim N(0, 1)$ ,  $\epsilon_t \sim t_4$ ,  $\epsilon_t \sim SN(\alpha = 1)$  and  $\epsilon_t \sim ST(\mu = 0, \sigma = 1, \alpha = 1, v = 4)$ . The corresponding boxplots of all the simulations are presented on Figure 16.

First, we consider Gaussian AR(2) processes, i.e.  $\epsilon_t \sim N(0, 1)$ . The Whittle's estimator always scores better in terms of MSE, bias and variance for both parameters (see Table 5). The estimator with results roughly similar to the state-of-the art estimator is the minimum weighted Wasserstein estimator. Unlike the others which have a high variance and, consequently, a high MSE.

Distribution	Gaussian					
	$\widehat{MSE}(\hat{\theta}^*)$		$\widehat{Bias}(\hat{\theta}^*)$		$\widehat{Var}(\hat{\theta}^*)$	
	$\phi_1$	$\phi_2$	$\phi_1$	$\phi_2$	$\phi_1$	$\phi_2$
$\hat{\theta}_{Whittle}^*$	0.000279	0.000308	-0.001944	0.000154	0.000276	0.000309
$\hat{\theta}_{MWE}^*$	0.005119	0.007030	-0.012938	0.030338	0.004964	0.006125
$\hat{\theta}_{MMWE, k=50}^*$	0.003132	0.003166	-0.007961	0.011897	0.003077	0.003032
$\hat{\theta}_{MSWE}^*$	0.003974	0.004072	-0.010912	0.013176	0.003864	0.003909
$\hat{\theta}_{MWE}^*$	0.000383	0.000449	-0.002598	0.000442	0.000377	0.000450

**Table 5:** Mean Squared Error / Bias / Variance of Figure 16 top plots.

In the scenario where the process distribution is heavy tailed, here Student t distribution, all MSE values of our new estimators decrease (see Table 6). As we can see on Figure 16, the boxplots cluster much more around the true value. As before, estimators converge faster to the true value of the parameter when the probability of getting very large values is higher than the standard normal distribution. The Whittle's estimator continues to achieve the best performance in terms of MSE.

Distribution	Student t					
	$\widehat{MSE}(\hat{\theta}^*)$		$\widehat{Bias}(\hat{\theta}^*)$		$\widehat{Var}(\hat{\theta}^*)$	
	$\phi_1$	$\phi_2$	$\phi_1$	$\phi_2$	$\phi_1$	$\phi_2$
$\hat{\theta}_{Whittle}^*$	0.000321	0.000281	-0.00117	-0.001100	0.000321	0.000281
$\hat{\theta}_{MWE}^*$	0.002953	0.003386	-0.005827	0.014389	0.002934	0.003195
$\hat{\theta}_{MMWE, k=50}^*$	0.000612	0.000586	-0.000508	-0.001591	0.000615	0.000586
$\hat{\theta}_{MSWE}^*$	0.000324	0.000281	-0.001093	-0.001109	0.000325	0.000281
$\hat{\theta}_{MWE}^*$	0.000438	0.000400	-0.001415	-0.000151	0.000438	0.000402

**Table 6:** Mean Squared Error / Bias / Variance of Figure 16 second plot from the top.

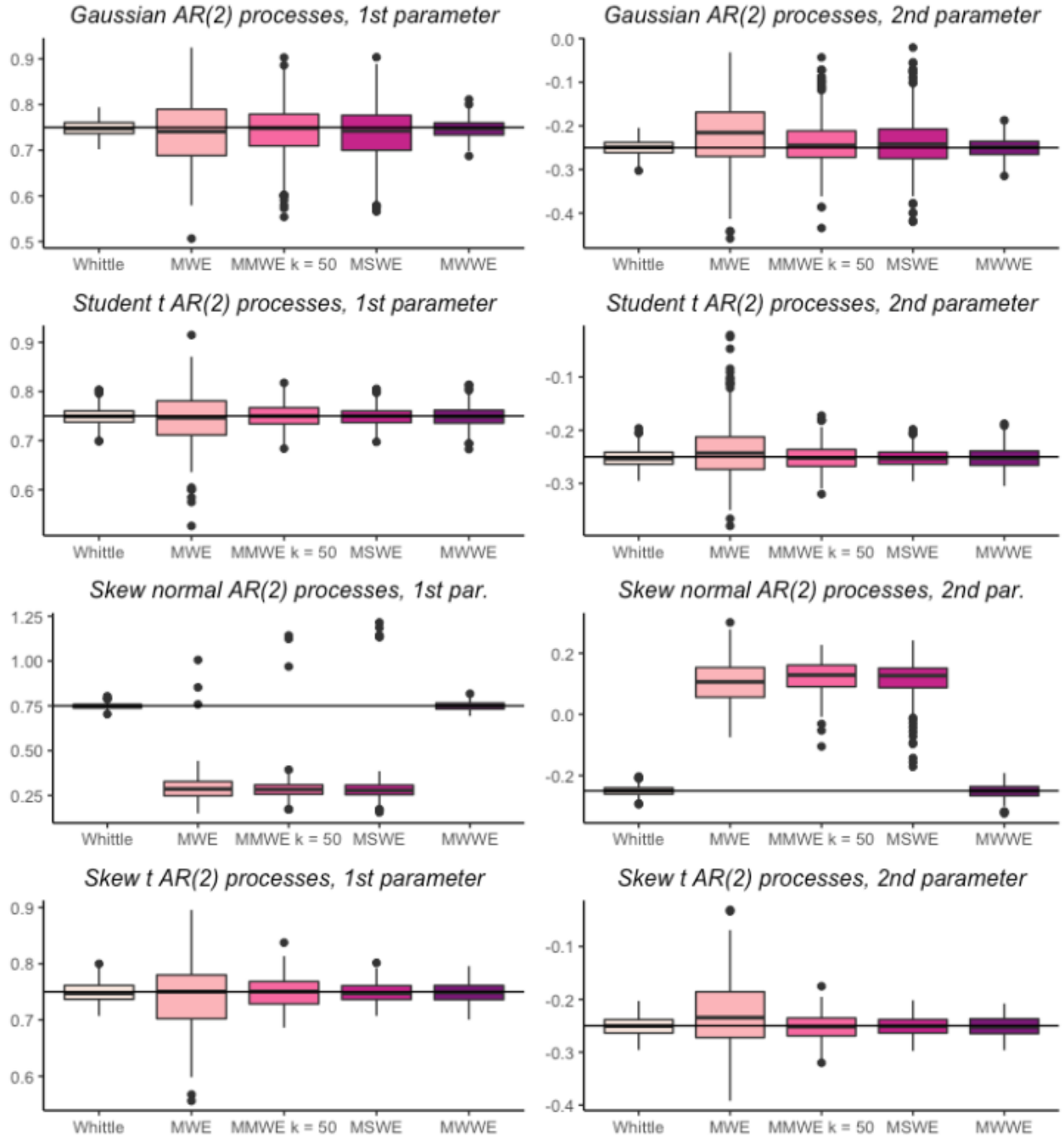


**Figure 16:** Boxplots of the Whittle's estimator, MWE, MSWE, MMWE, MWWE for 200 AR(2) processes. The left column is the first parameter (0.75) of the process, the right one is for the second parameter (-0.25).

On the other hand, contrary to long-memory processes, we observe that the fact that the underlying distribution are skewed or not is not relevant during the estimation procedure of the Whittle's estimator. Indeed, we do not perceive any bias in the Whittle's estimator in Figure 16 (third plot from the top) which is confirmed in Table 7. Regarding the estimators based on the Wasserstein distance we can observe a bias when the underlying distribution is a skew normal one. As soon as we raise the kurtosis of the distribution by means of the skew t distribution this bias disappears (see the bottom plot of Figure 16 and Table 8). As for the minimum weighted Wasserstein estimator, it remains consistent with the Whittle's estimator and is always very similar to it.

Distribution	Skew normal					
	$\widehat{MSE}(\hat{\theta}^*)$		$\widehat{Bias}(\hat{\theta}^*)$		$\widehat{Var}(\hat{\theta}^*)$	
	$\phi_1$	$\phi_2$	$\phi_1$	$\phi_2$	$\phi_1$	$\phi_2$
$\hat{\theta}_{Whittle}^*$	0.000269	0.000258	-0.001515	0.000316	0.000268	0.000257
$\hat{\theta}_{MWE}^*$	0.214071	0.131399	-0.452852	0.355448	0.009041	0.000554
$\hat{\theta}_{MMWE, k=50}^*$	0.218021	0.141375	-0.454870	0.371929	0.011169	0.003059
$\hat{\theta}_{MSWE}^*$	0.220240	0.136362	-0.446864	0.363478	0.020656	0.004267
$\hat{\theta}_{MWWE}^*$	0.000548	0.000554	-0.000497	-0.000933	0.000546	0.0.000552

**Table 7:** Mean Squared Error / Bias / Variance of Figure 16 third plot from the top.

Distribution	Skew t					
	$\widehat{MSE}(\hat{\theta}^*)$		$\widehat{Bias}(\hat{\theta}^*)$		$\widehat{Var}(\hat{\theta}^*)$	
	$\phi_1$	$\phi_2$	$\phi_1$	$\phi_2$	$\phi_1$	$\phi_2$
$\hat{\theta}_{Whittle}^*$	0.000321	0.000306	-0.001068	-0.000779	0.000321	0.000307
$\hat{\theta}_{MWE}^*$	0.003282	0.005058	-0.009552	0.021269	0.003206	0.004629
$\hat{\theta}_{MMWE, k=50}^*$	0.000705	0.000634	-0.000656	-0.000937	0.000708	0.000634
$\hat{\theta}_{MSWE}^*$	0.000319	0.000303	-0.001133	-0.000854	0.000319	0.000304
$\hat{\theta}_{MWWE}^*$	0.000373	0.000397	-0.000370	-0.001441	0.000375	0.000398

**Table 8:** Mean Squared Error / Bias / Variance of Figure 16 bottom plot.

In order to explain why a bias appears when  $\epsilon_t \sim SN(\alpha)$  and does not appear when we consider  $\epsilon_t \sim ST(\alpha, \nu)$ , we compute the Wasserstein loss of an AR(1) process  $Y_t = \phi_1 Y_{t-1} + \epsilon_t$  where  $\phi_1 = 0.6$  and  $\epsilon_t \sim SN(\alpha = 0.1)$  in the left plot of Figure 17 and  $\epsilon_t \sim ST(\alpha = 0.1, \nu = 4)$  in the right plot. By introducing an excess of kurtosis, thanks to the skew t distribution, we are facing a smooth Wasserstein loss. The convexe shape of the Wasserstein loss around the minimum value (see Figure 17 left plot) in the case of a skew normal distribution induces a bias in the parameter estimation.

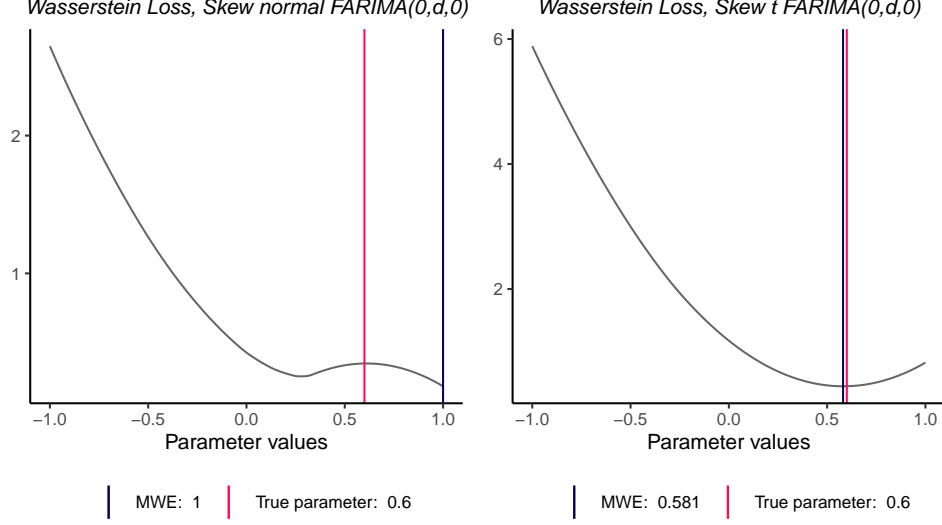


**Figure 17:** Wasserstein loss function of two  $AR(1)$  process with underlying distribution being a skew normal distribution and a skew  $t$  distribution. The sample size is equal to 3001

### 5.1.5 Additive Outliers : Short-Memory

We also replicate our experiment presented above by introducing some occasional outliers in a Gaussian  $AR(1)$  process

$$Y_t = 0.6Y_{t-1} + \epsilon_t$$

As a reminder, we contaminate the 200 simulated processes by means of the following equation:

$$Y_t = (1 - W_t) X_t + W_t (c \cdot V_t)$$

where  $W_t \sim \text{Bern}(p)$ ,  $V_t \sim t_2$  and  $c = 10$ . We let the value of  $p$  vary and evaluate the performance with three different ratios between the Whittle's estimator and the minimum weighted Wasserstein estimator: MSE ratio, bias ratio and variance ratio. The results are listed in Table 9. We observe the same kind of effect as for the long-memory process. Indeed, our minimum weighted Wasserstein estimator outperforms the Whittle's estimator when the process is contaminated. This improvement is due to the bias and variance both being smaller for the minimum weighted Wasserstein estimator for  $p < 0.05$ . Then, when  $p \geq 0.05$ , the minimum weighted Wasserstein estimator has a larger variance than the Whittle's.

p	0	0.001	0.01	0.05
MSE ratio	0.753	1.282	1.089	1.010
Bias ratio	0.905	1.107	1.044	1.005
Variance ratio	0.749	1.327	1.0589	0.813

**Table 9:** *MSE / Bias / Variance of the Whittle’s estimator divided by the MSE / bias / variance of the MWWE. The number of simulated AR(1) processes is equal to 200 with sample size equal to 3001. The innovation term is distributed according to a standard normal distribution.*

## 6 Conclusion

In this thesis, we introduce five new estimators that are based on minimum distance/divergence estimation. Our results suggest that we can outperform the state-of-the art estimation procedure when we are dealing with long-memory processes that have skewed underlying distributions. Moreover, it seems that our minimum weighted Wasserstein estimator can also be more efficient when short- and long-memory processes are contaminated by occasional outliers. In the case of short memory processes, we have similar results to Whittle’s estimator in terms of MSE. Through this thesis, we open the possibility for further research directions. An important step is to provide the theoretical understanding of our new estimators, studying e.g., consistency, asymptotic normality and robustness.

## References

- Ambrosio, Luigi, and Nicola Gigli. 2013. “A User’s Guide to Optimal Transport.” In *Modelling and Optimisation of Flows on Networks*, 1–155. Springer.
- Arjovsky, Martin, Soumith Chintala, and Léon Bottou. 2017. “Wasserstein Generative Adversarial Networks.” In *International Conference on Machine Learning*, 214–23. PMLR.
- Azzalini, Adelchi, and Antonella Capitanio. 2003. “Distributions Generated by Perturbation of Symmetry with Emphasis on a Multivariate Skew t-Distribution.” *Journal of the Royal Statistical Society: Series B (Statistical Methodology)* 65 (2): 367–89.
- Bassetti, Federico, Antonella Bodini, and Eugenio Regazzini. 2006. “On Minimum Kantorovich Distance Estimators.” *Statistics & Probability Letters* 76 (12): 1298–1302.
- Basu, Ayanendranath, Hiroyuki Shioya, and Chanseok Park. 2019. *Statistical Inference: The Minimum Distance Approach*. Chapman; Hall/CRC.
- Beran, Jan. 1994. *Statistics for Long-Memory Processes*. Vol. 61. CRC press.
- Bernton, Espen, Pierre E Jacob, Mathieu Gerber, and Christian P Robert. 2019. “On Parameter Estimation with the Wasserstein Distance.” *Information and Inference: A Journal of the IMA* 8 (4): 657–76.
- Brillinger, David R. 2001. *Time Series: Data Analysis and Theory*. SIAM.
- Cuturi, Marco. 2013. “Sinkhorn Distances: Lightspeed Computation of Optimal Transport.” *Advances in Neural Information Processing Systems* 26: 2292–2300.
- Friedman, Jerome, Trevor Hastie, Robert Tibshirani, and others. 2001. *The Elements of Statistical Learning*. Vol. 1. 10. Springer series in statistics New York.
- Gourieroux, Christian, and Alain Monfort. 1995. *Statistics and Econometric Models*. Vol. 1. Cambridge University Press.
- Kantorovich, Leonid V. 1942. “On the Translocation of Masses.” In *Dokl. Akad. Nauk. USSR (NS)*, 37:199–201.
- Kolouri, Soheil, Se Rim Park, Matthew Thorpe, Dejan Slepcev, and Gustavo K Rohde. 2017. “Optimal Mass Transport: Signal Processing and Machine-Learning Applications.” *IEEE Signal*

- Processing Magazine* 34 (4): 43–59.
- Mikosch, Thomas, Tamar Gadrich, Claudia Kluppelberg, and Robert J Adler. 1995. “Parameter Estimation for ARMA Models with Infinite Variance Innovations.” *The Annals of Statistics*, 305–26.
- Monge, Gaspard. 1781. “Mémoire Sur La Théorie Des déblais Et Des Remblais.” *Histoire de l’Académie Royale Des Sciences de Paris*.
- Ni, Hao, Lukasz Szpruch, Magnus Wiese, Shujian Liao, and Baoren Xiao. 2020. “Conditional Sig-Wasserstein GANs for Time Series Generation.” *arXiv Preprint arXiv:2006.05421*.
- Panaretos, Victor M, and Yoav Zemel. 2020. *An Invitation to Statistics in Wasserstein Space*. Springer Nature.
- Peyré, Gabriel, Marco Cuturi, and others. 2019. “Computational Optimal Transport: With Applications to Data Science.” *Foundations and Trends in Machine Learning* 11 (5-6): 355–607.
- Priestley, Maurice Bertram. 1981. *Spectral Analysis and Time Series: Probability and Mathematical Statistics*. 04; QA280, P7.
- Santambrogio, Filippo. 2015. “Optimal Transport for Applied Mathematicians.” *Birkhäuser, NY* 55 (58-63): 94.
- Tsay, Ruey S. 2005. *Analysis of Financial Time Series*. Vol. 543. John wiley & sons.
- Villani, Cédric. 2009. *Optimal Transport: Old and New*. Vol. 338. Springer.
- Whittle, Peter. 1953. “Estimation and Information in Stationary Time Series.” *Arkiv för Matematik* 2 (5): 423–34.